Bioorganic Chemistry 93 (2019) 103308

Contents lists available at ScienceDirect

Bioorganic Chemistry

journal homepage: www.elsevier.com/locate/bioorg

A mass spectrometric stochastic dynamic diffusion approach to selective quantitative and 3D structural analyses of native cyclodextrins by electrospray ionization and atmospheric pressure chemical ionization methods

Bojidarka Ivanova*, Michael Spiteller

Lehrstuhl für Analytische Chemie, Institut für Umweltforschung, Fakultät für Chemie und Chemische Biologie, Universität Dortmund, Otto-Hahn-Straße 6, 44221 Dortmund, Nordrhein-Westfalen, Germany

ARTICLE INFO

Keywords:
Mass spectrometry
Diffusion
Quantum chemistry
Cycloidextrins
Carbohydrates

ABSTRACT

The paper addressed shortcoming with highly precise and selective 3D structural analysis of native cyclodextrins in mixture using ions observable at low *m/z*–region by ESI– and APCI–mass spectrometry. Because of, the quantitative and structural analyses of CDs, in general, are vexed by a set of complications. The study outlines our own stochastic dynamic approaches to the latter issues based on new model relations, quantifing the measurable MS outcome *intensity*. They introduce the so–called *stochastic dynamic mass spectrometric diffusion* "D_{SD}" parameter, exhibiting high accuracy, precision, sensitivity and selectivity, respectively. It is linearly connected with the so–called *quantum chemical diffusion parameter* "D_{QC}" according to Arrhenius's theory. The most important upshot is that statistical parameters $r = 0.99_{639}$–0.99_{981} has been obtained correlating between D_{SD} and D_{QC} parameters. Therefore, we determine high accurately 3D molecular and electronic structures of analytes by mass spectrometry. Fragment peaks at *m/z* 313, 279, 272, 252, 231, 214, 198, 171, 158 and 141 are examined. Mixtures of CDs and monomeric and acyclic oligomer carbohydrates glucose (1), sucrose (2), raffinose (3), melezitose (4) and cellotriose (5) are also studied. Our method is able to account precisely for the effect of the temperature under ESI– and APCI–MS conditions, as well. Correlative analysess between D_{SD} parameters of ESI– and APCI–MS measurements under different temperatures is also shown. Chemometric tests are used. Another important results and conclusions, among others, to draw from this research are: *(i)* excellent linear correlation between D_{SD} and D_{QC} parameters of $r = 0.99_{636}$ is found looking at common ions at *m/z* 141, 158 and 171, belonging to 2-formyl-3,4-dihydroxy-pyranylium, 4,5,6-trihydroxy-6H-pyran-2-carbaldehyde and 3,4,5-trihydroxy-6-oxo-6H-pyran-2-ylmethylidyne-oxonium ions. Thus, we distinguish precisely between the last structure and 3-formyl-4,5-dihydroxy-2,7-dioxa-8-oxonia-bicyclo[4.2.0]octa-1(8),3,5-triene cation. In the case of ion at *m/z* 141 subtle electronic effects are distinguished between the mentioned structure and the charged 3,4-dihydroxy-6H-pyran-2-carbaldehyde one. The method determines precisely very similar structurally poly–OH–substituted derivatives. Because of, *(ii)* absolute reproducibility ($r = 1$) of D_{SD} parameters of ESI–MS spectra is obtained studying the shown in point *(i)* MS peaks of β-CD between j^{th} and j^{th} numbers of experiments. The statistical equation is $D^{i}_{SD} = (0.51 \pm 3.1.10^{-5}) \times D^{j}_{SD}$; *(iii)* the APCI– and ESI–MS provide identical results studying common MS ions of CDs and the correlation between D^{APCI}_{SD} and D^{ESI}_{SD} parameters excludes from error, due to, experiment; and *(iv)* The correlation between theory and experiment accounting for the factor *temperature* within our model equations shows $r = 0.98_{28}$ looking at the MS peaks at *m/z* 313 280, 279, 274 and 252, respectively. The effect of the temperature under both ESI– and APCI–MS conditions on the 3D molecular and electronic structures of CDs is precisely studied, respectively.

Abbreviations: APCI, atmospheric pressure chemical ionization; BO, Born, Oppenheimer; CB, carbohydrate; CD, cyclodextrin; CID, collision induced dissociation; DFT, density functional theory; D_{SD}, stochastic dynamic mass spectrometric diffusion parameter; D_{QC}, quantum chemical diffusion parameter; D_{CMM}, diffusion parameter according to current monitoring method; ESI, electrospray ionization; *m/z*, mass–to–charge; MD, molecular dynamics; MS, mass spectrometry; SD, stochastic dynamics; SD*, standard deviation; LMW, low molecular weight; TD, thermodynamics; TIC, total ion current; TOF, time–of–flight

* Corresponding author.
E-mail addresses: B.Ivanova@infu.uni-dortmund.de, B.Ivanova@web.de (B. Ivanova).

https://doi.org/10.1016/j.bioorg.2019.103308
Received 27 March 2019; Received in revised form 19 August 2019; Accepted 19 September 2019
Available online 20 September 2019

1. Introduction

The native (α–, β – and γ–) cyclodextrins are attractive templates studying host–guest interactions [1,2]. The straightforward understanding of these interactions incorporates into a detailed study the bonding fashions and strengths of molecular forces. These analytes exhibit a large number of different molecular conformations and interacting network of monomers, oligomers, polymers and supramolecular self–associates, respectively. This fact, complicates the structural analysis by mass spectrometry. In general, the soft ionization MS methods are irreplaceable approach to examine biomacromolecules, their noncovalent interactions [3–5]. Research on reactions of protonation/deprotonation in gas– and condense phases or noncovalent interactions of LMW analytes or both, in addition to, analysis of biologically active macromolecules [6–18] have been documented. Looking at the studies of CBs, so far, it should be borne in mind that MS based examination of such compounds is a well-established field of the *analytical chemistry* [8–18]. However, one important conclusion can be drawn from the literature, so far. The structural analysis has been limited to 2D molecular structures (Scheme SA1). Certainly, this could be interesting in interdisciplinary application to mass spectrometry. However, such structure lacks of providing crucial information about 3D conformation; bond lengths and angles; electronic structure and effects; nature of chemical bonds, information about chemical reactivity, etcetera. It immediately might be suggested what our contribution basically consists in. We have sought to demonstrate how ESI– and APCI–methods can be used to determine 3D molecular and electronic structures of CDs looking at fragment ions at low *m/z*–values. It remains to be seen, in practice, how this can be carried out. We shall briefly introduce our own more recent developments treating the measurable outcome *intensity*, quantitatively. It is useful for an in–depth understanding of the method to show how the new SD model Eq. (1) accounts for different 3D conformations or electronic structures or both corresponding to one and the same *m/z* value of the spectra (Figs. 1 and 2). There are depicted calculation tasks of D_{SD} parameters, formulas and statistical equations connecting D_{SD} data of i^{th} and j^{th} experiments of isolated analytes and their mixtures. The significant importance of the data lies in that they distinguish quantitatively between analytes using a set of identical MS ions. Under one and the same experimental conditions, the relation among D_{SD} parameters of isolated analytes is different from corresponding values of mixtures, chemometrically. The D_{SD} parameter accounts sensitively for any perturbation of the variable *intensity per* span of scan time. But, what is the physical meaning of perturbation or change of the parameter D_{SD} and how the change/perturbation, if any, is connected with 3D molecular structure of the ions? Eq. (1) [19–26] connects MS intensity of i^{ts} analyte ion within a given j^{th} span of scan time of a MS experiment with a parameter D_{SD}. The D_{SD} parameters correspond linearly to D_{QC} parameters (Eqs. (6)–(8) [24]). Owing to that D_{QC} parameter reflects unique 3D molecular and electronic structures of an analyte, the formalism behind Eq. (1) provides direct connection of D_{SD} with 3D conformation and electronic structure of the molecules. One advantage of Eq. (1), among others, consists of its significant sensitivity. The model is exploited, so far, studying organic and metal–organics of LMW and biomacromolecules [19–26]. Herein, we employ Eq. (1) for CDs and their mixtures with CBs (1)–(5), thus, solving significantly challenging problems of determining such analytes using ions having low *m/z*–values.

2. Experimrntal

2.1. Materials and methods

Mass spectrometric analysis was performed by means of Thermo Finnigan LTQTune 391, Thermo Finnigan LTQ Orbitrap (Thermo Fisher Inc., Rockville, MD, USA) and Agilent 1200 G1315 DAD (Agilent Technologies Inc., SC, USA) The following columns were used: Fusion RP 80–150 × 2 and Fusion 150 × 3. A combination of mass detectors was used. The data were saved as individual files. The MS intensities were processed by QualBrowser 2.7, ProteoWizard 3.0.11565.0 (2017) and AMDIS 2.71 (2012) program packages. Tables AS1, AS2 and BS1 show the experimental conditions of ESI– and APCI–MS measurements. The chromatograms were obtained by Gynkotek (Germering, Germany) HPLC instrument having a preparative Kromasil 100 C18 column (250 × 20 mm, 7 μm; Eka Chemicals, Bohus, Sweden) and a UV detector set at 250 nm. The MS are correlated with UV–VIS ones.

The CBs were Sigma–Alrdich products.

2.2. Sample preparation for ESI– and APCI–MS measurements

2.2.1. Preparation of the samples

Standard solutions of CDs were prepared daily in mobile phase CH_3CN:CH_3OH (25:75, *v/v*) in multiplication (samples 01–06 of β–CD; samples A_1–F_1 of α–CD; and samples A_1 and B_1 of γ–CD). They were homogenized for 10 min at 1500 $r{\cdot}min^{-1}$ with shaker. The solutions stored in the dark at –4 °C. Aliquots were measured under ESI– and APCI–MS conditions. The analyses of LMW CBs were based on samples 01–09. The hydrolysis of CBs was carried out within a range pH = 7–14 recalculated for solvent mixture using standard solutions of NH_4OH and NaOH.

2.2.2. Linearity and quantitation limits

The linear range has been determined by standard CDs and CBs by diluting of solutions of 1.0 $\mu g{\cdot}(mL)^{-1}$ of each compound in solvent mixture CH_3CH_2OH:H_2O at molar ratio 1:1 within concentration ranges: 01–50 $ng{\cdot}(mL)^{-1}$ to 0.05–5000 $\mu g{\cdot}(L)^{-1}$. The quantitation concentration limits has been obtained.

2.2.3. Accuracy and precision

The accuracy has been evaluated using three replicates of CDs and solvent mixture CH_3CN:H_2O at molar ratios 1:1 at concentrations of 2 $\mu g{\cdot}(mL)^{-1}$. Three subsequent measurements of the samples were carried out. The precision has been estimated by five sequent (three times repeated) measurements of standard samples of CDs.

2.2.4. Intermediate precision conditions of measurements

The intermediate precision conditions of measurements can be interpreted as a set of conditions, including identical measurements procedures and replicate measurements over an extended span of the time. They may include different conditions involving changes, for instance, different operators. Measurements over different spans of time have been carried out.

2.2.5. Trueness of measurements and bias

The closeness of agreement with average data has been obtained by means of replicated measurements (twelve measurements) and compared with the true value of reference samples. The measurement trueness is inversely related to SME, which estimated the measurement bias.

2.2.6. Repeatability and reproducibility

The *repeatability* and *reproducibility* of measurements is evaluated using the following procedure: *(i)* data of three repeated measurements of three replicated samples have been collected and compared with standards; and *(ii)* chemometric analysis has been carried out [19–33]. The convention of *repeatability* and *reproducibility* has been detailed [33]. The statistical parameters are determined by means of the following formulas: $2{\cdot}(2)^{1/2}{\cdot}SD_1$ and $2{\cdot}(2)^{1/2}{\cdot}SD_2$, where SD_1 and SD_2 represent short time standard deviation (SD) and the long-time SD.

2.2.7. Recovery

Recovery has been evaluated by standard method, using ten portions of CDs samples with different ratio (2.0 $\mu g{\cdot}(mL)^{-1}$) at different high,

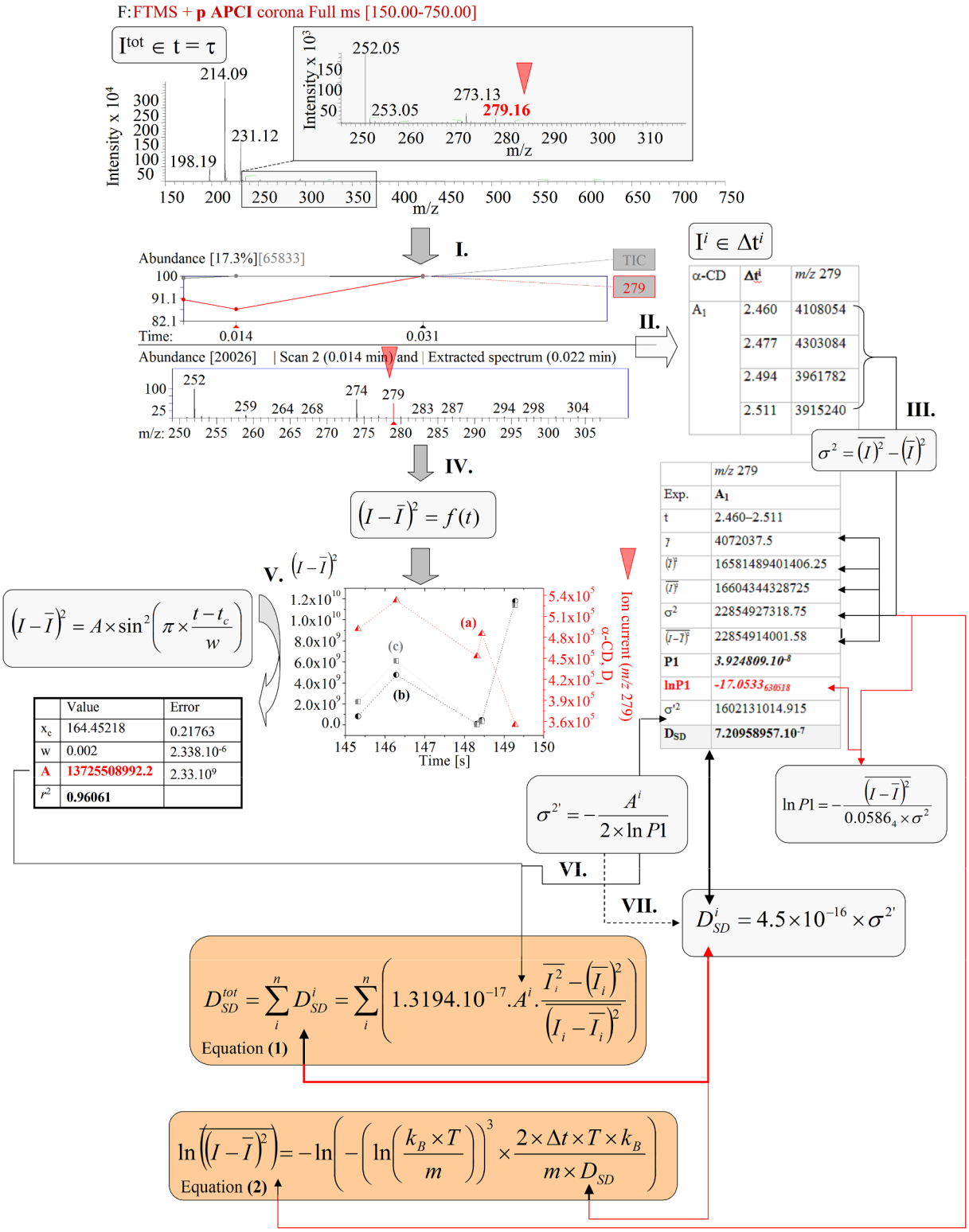

Fig. 1. Schematic representation of tasks (I–VII) and formulas for calculation of D_{SD} values according to [19–26]; a measured MS spectrum (upper figure) contains information about total intensity of ions (I^{tot}, [arb.units]) which is summed up over the whole scan time (t = τ = 17–30 mins); tasks I and II: determination of temporal behavior of absolute intensity I^i over a i^{th} short span of the scan time Δt [mins]; task III: determination of the average intensity over i^{th} span of time, variance parameter σ^2 and lnP1; task IV: plotting of functional relationship $(I - \langle I \rangle)^2 = f(t)$; task V: SineSqr fitting of the latter relation and determination of parameter "A"; task VI: determination of σ'^2 variance parameter; and task VII: determination of D^i_{SD} parameter [$cm^2 \cdot s^{-1}$] over i^{th} span of measurement time (Experimental files a-CD.raw and rb01.raw able to follow the computational tasks).

intermediate and low concentrations. In parallel, they were splitted into different concentration groups: 35, 7.5, 2.5 $ng \cdot g^{-1}$, respectively. Three additional portions have been selected as controls. All recoveries show good method accuracy.

2.3. Theory/computations

2.3.1. Computational quantum chemistry (Supporting information)

2.3.1.1. Stochastic dynamics. Eq. (1) has been obtained by adopting the

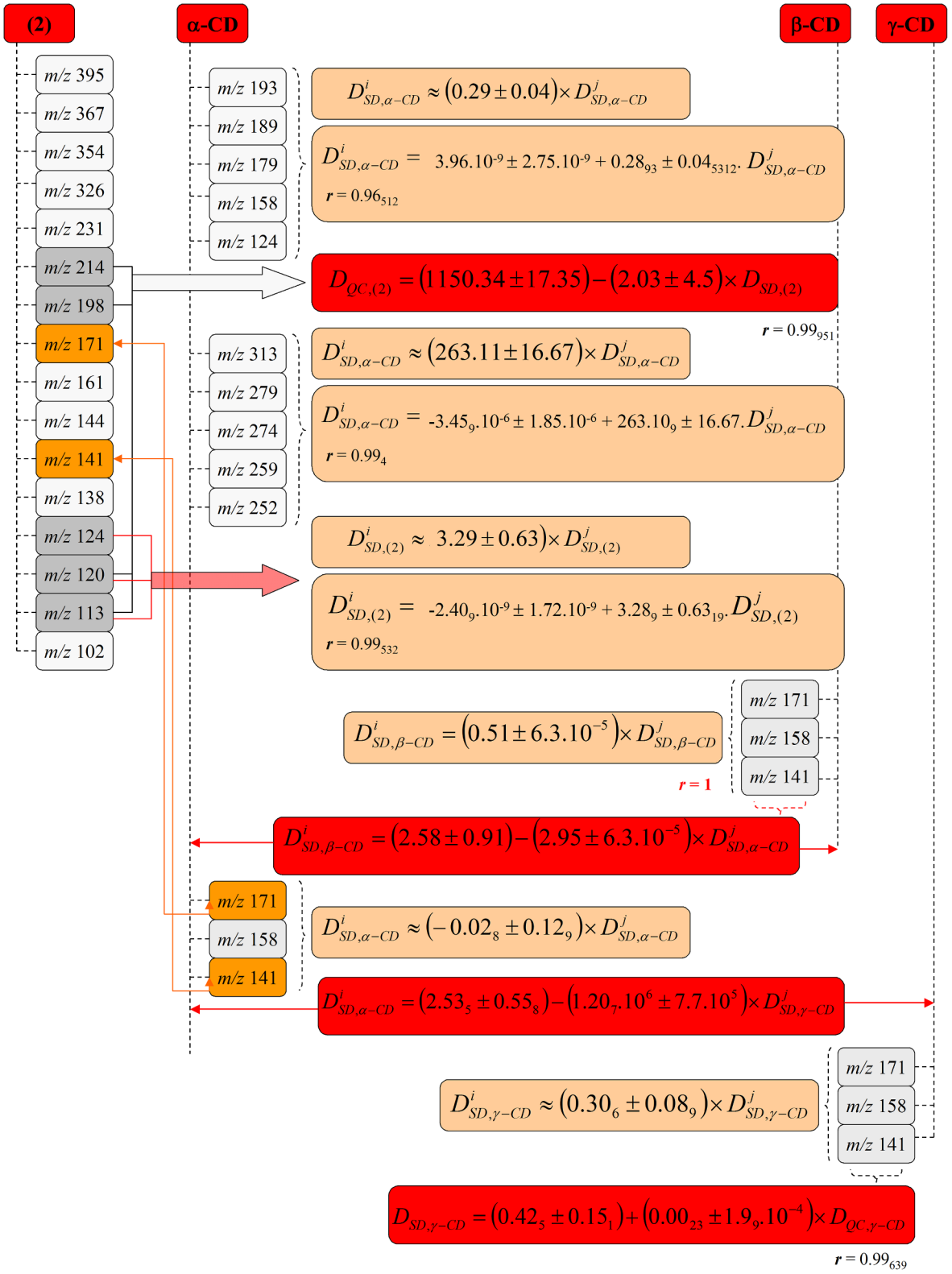

Fig. 2. Characteristic MS fragment peaks of CDs and (2); statistical equations connecting D_{SD} parameters of isolated analytes under i^{th} and j^{th} experimental conditions with those of mixtures; statistical equations connecting D_{SD} [$cm^2 \cdot s^{-1}$] with D_{QC} parameters.

Box–Müller's method and the Ornstein–Uhlenbeck approximation to SD processes [19–26]. It represents a purely SD approach. The experimental measurable outcome *intensity* from a MS experiment is treated as a stochastic variable. The absolute intensity value with respect to different spans of measurement's the scan time is quantified. According to the stochastic plausibility theories any stochastic variable or variation of absolute value of MS intensity with respect to the time and its average value *per* a concrete span of time (in this case, different spans of the scan time) are connected with the so–called *variance* "σ^2" (Fig. 1(III)). We study both of these experimental and theoretical

functional relations $(I–\langle I\rangle)^2 = f(t)$. The former relation can be approximated to SineSqr function at an absolute level of statistical significance, thus producing the latter relation (Fig. 1(V)). The nonlinear approximation to experimental relation $(I–\langle I\rangle)^2 = f(t)$ results in excellent or even absolute coefficients of statistical correlation ($r^2 = 1$). Due to, chemometric nonlinear fitting of experimental $(I–\langle I\rangle)^2 = f(t)$ relation the variance of the theoretical relation (σ'^2) should be different from the experimental variance σ^2. The D_{SD} parameter accounts for error contribution to chemometric data processing *via* $\sigma^{2'}$ parameter (Consider Fig. 1(VII)). A second note is associated with quantitative procedure of the temporal behavior of the MS intensity consist in evaluating differences in intensity with respect to the experimental parameter temperature (T), as far as, the experimental design is based on ESI and APCI MS measurements under different experimental conditions toward the temperature. After having introduced the basic concept of quantitative treatment of MS intensity *via* the D_{SD} parameter and Eq. (1), we will concentrate on the concept of the functional relation between the D_{SD} parameter and the temperature given by Eq. (2) [26]. It adopts the Gillespie's exact numerical solution of the forward Fokker–Planck equation or forward Kolmogorov equation of an Ornstein–Uhlenbeck process. In writing Eq. (2) we adopt, as well as, the Einstein's formula of the characteristic function for drift (see Eq. (4) in [26]). However, we modify empirically the characteristic function of the diffusion in the forward Fokker–Planck equation (see Eq. (5) in [26]). In Eq. (2), k_B denotes the Boltzmann constant ($1.3806.10^{-23}$ $m^2{\cdot}kg{\cdot}s^{-2}{\cdot}K^{-1}$); $\Delta t = t - t_0$, T – temperature [K] under the two ESI and APCI measurements; m – mass and D is the diffusion coefficient corresponding to D_{SD} according to Eq. (1), respectively.

2.4. Chemometrics

The software R4Cal Open Office STATISTICs for Windows 7 was used. The statistical significance was checked by *t*-test. The model fit was determined upon by F-test. ANOVA test was also used. The nonlinear fitting of experimental MS data was carried out by means of searching method based on Levenberg-Marquardt algorithm [19–33].

3. Results

3.1. Accuracy and precision of the mass spectrometric measurements

The error of measurements contributes to the accuracy of the D_{SD} data. Figs. AS1–AS9 (Appendix A) depicts ESI– and APCI–MS spectra of analytes (samples 01–06). The descriptive statistics yields to mean value = 252.04557, sd*(yEr ±) = $5.7735.10^{-5}$, se(yEr ±) = $3.33333.10^{-5}$; 214.0898, sd*(yEr ±) = 0, se (yEr ±) = 0; and 231.1163, sd*(yEr ±) = 0, se(yEr ±) = 0. The sd*(yEr ±) is equal to "zero" comparing among CDs. The same is true for, analysis of experimental parameters of ESI– and APCI–MS spectra. The chemometrics shows a lack of contribution of error of measurements to the D_{SD} values. The APCI– and ESI–MS provide identical results. The *m/z*– and intensity values have identical accuracy. The correlation between D_{SD}^{APCI} and D_{SD}^{ESI} parameters excludes from error, due to, experiment.

The chemometrics of MS peaks at *m/z* 113.07, 198.19 and 231.12 of samples 01–09 of CBs (1)–(5) (Figs. BS3–BS10, Table BS1) under APCI–MS conditions show accuracy: mean value = 113.07102, sd*(yEr ±) = $4.40959.10^{-5}$, and se(yEr ±) = $1.47.10^{-5}$; 198.1853, sd*(yEr ±) = 0, and se(yEr ±) = 0; and 231.1161, sd(yEr ±) = 5.10^{-5}, and se(yEr ±) = $1.67.10^{-5}$, respectively. Table BS2 shows ANOVA results. The F value is almost zero (F ≈ 8.10^{-13}). The P value is equal to 1.

The method performances of measurements of *m/z*–values are depicted in Fig. CS1 and summarized in Table CS1 (Appendix C).

3.2. Mass spectrometric data of mono–and acyclic oligosaccharides – qualitative analysis

The fragment patterns of the CDs under ESI(-)–MS operation mode within low *m/z*–charge range has shown virtually identical isotope shapes. Characteristic MS peaks at *m/z* 179, 161, 149, 143, 131, 119 occur. Peaks at *m/z* 113 (1) and 341 (2) are found [34] (Figs. BS3–BS10). Looking at the molecular structures of ions at *m/z* 161 and 143, it is evident an intramolecular rearrangement. The pairs of structures (Figs. BS1 and BS2) m_{144_a}/m_{144_b}, m_{161_a}/m_{161_b} and m_{231_a}/m_{231_b} can belong to peaks at *m/z* 144, 161 and 231 in the spectra of (1) and (2). An intramolecular rearrangement causes for an equal possible observation of either m_{144_a} or m_{144_b}; m_{161_a} or m_{161_b}; or m_{231_a} or m_{231_b} in the spectra. Therefore, a reliable structural analysis is associated with a number of critical aspects. The first and most important aspect is that, within complex CB scaffolds there can be assigned more than one molecular structure to given MS peak. CBs exhibit great chemical reactivity and produce a number of oligomers and polymers *via* α(1–2) to α (1–6) and β(1–2) to β(1–6) bonds [35–41]. Figs. BS3–BS12 reveals different product oligomeric ions. The MS peaks at *m/z* 326 and 214 figure on the type of the chemical bond of oligosaccharides. Ref. [35] has shown a preferred cleavage of glyosidic bond between second and third monomeric units. Our analysis focuses on competitive cleavage of glyosidic bond between the first and second, as well as, the second and third monomeric units of analytes (3)–(5). The dehydration reactions of cellulose yields to unsaturated CBs, having different location of the double bond [42,43]. The position of the OH group plays a significant role. The cleavage of substituent at C^2–OH position requires a significant amount of energy. It is observed in high temperatures. Nonetheless, it has been described as most preferred process comparing with a cleavage of C–O(H) bonds at C^3–OH and C^6–OH positions. The analysis of MS ion at *m/z* 326 shows that, the fragment products after cleavage of OH groups are: $m^{(6)}_{326\_d\_e}$, $m^{(6)}_{326\_d\_f}$ and $m^{(6)}_{236\_d\_h}$, respectively. Various mechanisms of pyrolysis of cellulose such as direct bond cleavage; retro–Diels–Alder reaction; C^6–OH pinacol reaction of cleavage and a retro–aldol process have been examined [37]. Two step mechanisms of reactions have been found as a highly probable one. The retro–Diels–Alder mechanism with $C^3 = C^2$–OH fragment is favourable [36]. We also propose a two-step mechanism of ions formation, in spite of; such mechanism does not occur frequently studying LMW analytes. The macromolecules often have shown parallel processes of proton transfer and intermolecular rearrangement [19–26].

The chromatographic data show that within pH = 1–9 there is insignificant amount of oligomer products (RTs = 13–16 mins). The most abundant MS peak at *m/z* 198 belongs to {[glucose + NH_4^+]} or an ammonium addict of (1) evidences that within latter pH values there is a lack of deprotonation of the analytes. These results agree excellent with nuclear magnetic resonance study of β–CD [41], showing a high stability of oligomer CBs within a large range of pH values.

3.3. Mass spectrometry of mono– and oligosaccharides – quantitative stochastic dynamic diffusion parameters

The determination of D_{SD} parameters is carried out (Fig. 1). First, *(i)* the absolute intensity of MS ions within low *m/z*–region of the spectra of 01–09 over spans of scan time is quantified (Figs. BS13–BS16 and Table BS3). Second, *(ii)* the values of intensity (I) (Table BS4) ($\langle I\rangle$, $\langle I\rangle^2$, $\langle(I)^2\rangle$and $\langle(I-\langle I\rangle)^2\rangle$) together with statistical parameter "A" and variance parameters σ^2 and $\sigma^{2'}$ are determined. The parameter $\ln P1 = -17.053_4$ is constant. The statistical parameter "A" is obtained by SineSqr approximation to experimental relationship $(I-\langle I\rangle)^2 = f(t)$ (Fig. BS17). The D_{SD} values are calculated according to the formulas shown above and data in the latter table. If the 3D molecular and electronic structure of a fragment ion does not change over the studied spans of scan time, then D_{SD} parameters correlate excellent (Figs.

BS18–BS20). The coefficients of correlations are $r > 0.99$. When, a perturbation (or change) of 3D molecular conformation or electronic structure of a MS ion over different spans of times occur, then the D_{SD} values vary. The total diffusion parameter (D_{SD}^{tot}) represents a sum up of $D_{SD}^{\Delta tn}$ parameters over the whole scan time. Major contribution to a 3D structure should have this $D_{SD}^{\Delta tn}$ parameter, which exhibits the largest value (Fig. BS21). If a set of 3D molecular structures have $D_{SD}^{\Delta tn} = 10^{-12}$–$10^{-14}$ over an average value $D_{SD}^{\Delta tn} \approx 10^{-4}$–$10^{-6}$ could be neglected from the description of the 3D structure of the cation. Table BS4 and Figs. BS18–BS20 highlight that within the shown an almost identical or strongly overlapped span of the times there is obtained perfect correlation between D_{SD} parameters of MS ions measured within independent experiments ($r = 0.99_9$–1). This fact explains the excellent reproducibility of APCI–MS data under one and the same experimental conditions (Table BS1). The superior reproducibility is typical not only determining *m/z* values – a well/ known fact – but the diffusion parameters. The results from D_{SD} parameters (Table BS4 and Figs. BS18–BS22) represent a rigours facts about: *(i)* reliability of our 3D assignment of MS ions; *(ii)* capability of Eq. (1) of treatment of MS intensity as a powerful tool not only for exact 3D structural analysis of ions, but also for its routine implementation into the analytical practice together with well/known methods treating the peak positions of MS ions; and *(iii)* high accuracy, precision and selectivity of so and structurally similar complex analytes such CBs.

Next, we shall draw attention to application of Eq. (1). So far, we have described quantitatively relatively small spans of time. A question arises: does Eq. (1) appear applicable to large scan time? Table BS2 illustrates absolute intensities of MS ions over larger spans of times. Figs. BS23–BS25 depicts experimental parameters and chemometrics. As can be seen (Table BS4) lnP1 is, again, the same constant equal to -17.053_4. The upshot of the latter analysis is that the equation is applicable to quantify small and large spans of the scan times.

3.4. Stochastic dynamic mass spectrometric diffusion parameters of native cyclodextrins – electrospray ionization mass spectrometric data

3.4.1. Stochastic dynamic mass spectrometric diffusion parameters of α–cyclodextrin

Table AS1, Fig. 2 and AS10–AS14 depict intensity of MS ions of α–CD over the scan time (t) under experiments A_1–F_1. Fig. AS1 illustrates fragment patterns and assignment of MS ions. Tables AS3–AS10 summarize absolute intensity *per* span of time of experiments A_1–D_1; experimental and statistical parameters according to Eq. (1) together with D_{SD} parameters. Fig. AS15 shows experimental relations between ion current *per* span of time; the experimental relation $(I–\langle I\rangle)^2 = f(t)$; its nonlinear approximation to SineSqr function; and chemomerics. Figs. AS16–AS19 depicts mutual relations between absolute total intensities of MS ions with respect to the experimental scan time (τ); and D_{SD} parameters of ions of α–CD. A set of experimental conditions labeled as A_1–F_1 are examined. The significant results go beyond the common view that CDs can be distinguished quantitatively only using ions at high *m/z*–values, where MS peaks of adduct $\{[\alpha\text{–CD} + NH_4]^+\}$, $\{[\beta\text{–CD} + NH_4]^+\}$ and $\{[\gamma\text{–CD} + NH_4]^+\}$ ions at $m/z = 990$–1400 occur. These peaks enable a highly selective determination of CDs even in complex multicomponent mixtures (Fig. 3, AS1–AS10 and AS19) by means of CID–MS analysis [6,7]. The CID–MS yields to relatively low fragment products, due to soft–ionization conditions. The product ions appear, again, within high *m/z*–region of the spectra (Figs. 4, 5, AS20 and AS21). However, the analysis of CID fragment ions of ammonium adducts of CDs becomes outside the basic idea of this study. Analysis within low *m/z*–values is undoubtedly a challenging research task, due to, complexity of ESI– or APCI–MS isotope shapes of CDs under single MS operation mode. However, the D_{SD} parameters are highly selective and allow for overcoming of the latter drawback of the experimental MS outcome.

3.4.2. Stochastic dynamic mass spectrometric diffusion parameters of β–cyclodextrin

We shall discuss experimental D_{SD} results from β–CD. Tables AS11 and AS12 summarize the temporal behavior of absolute MS intensity of ions with respect to a set of spans of scan time. The experimental MS spectra are depicted in Fig. AS21. The relations among TIC *per* span of the time; the function $(I–\langle I\rangle)^2 = f(t)$ and its nonlinear approximation to SineSqr function are presented in Fig. AS22. Figs. AS23 and AS24 illustrate correlative analysis among D_{SD} results from different experimental conditions A_1 and B_1; and between α–CD and β–CD measured under experimental conditions F_1 and E_1; and, respectively, A_1. The analysis encompasses ions at *m/z* 141, 158, 171 and 198, respectively. The *m/z*–values of the peaks at *m/z* 141 and 171 are identical in α– and β–CDs from the perspective of chemometrics (Fig. AS25, mean value: 141.1136, sd*(yEr ±) = se(yEr ±) = 0; and 171.1017, sd*(yEr ±) = se(yEr ±) = 0). As could be expected the D_{SD} parameters of these peaks of β–CD, like in α–CD, under independent experimental conditions A_1 and B_1 are identical. Absolute coefficient of correlation $r = 1$ has been obtained. However, as the latter figure clearly demonstrates, the analysis of D_{SD} data of the same MS peaks of α– and β–CD shows that these parameters do not correlate linearly at a significant level based on chemometric criterion ($r = 0.65_{626}$). As we have outlined above, the new approach to quantify MS intensity according to Eq. (1) and parameter D_{SD} exhibit high sensitivity towards any perturbation of 3D molecular conformation and electronic structures of ions. No of the existing quantitative methods for analysis neither of MS intensity nor *m/z*–parameters does not match our strategy. On the contrary, looking at protocols for determining analytes the fact that the MS peaks at *m/z* 171 and 141 show sd*(yEr ±) = se(yEr ±) = 0 means that these peaks cannot be detected selectively. However, Figs. AS23 and AS24 reveal that the analysis of D_{SD} data provides high selective determination of α– and β–CD. Because of, the corresponding correlations are expressed quantitatively *via* different statistical linear equations looking at the temporal behavior of absolute MS intensity *per* span of the scan time (Tables AS3, AS9–AS12 and CS1).

3.4.3. Stochastic dynamic mass spectrometric diffusion parameters of γ–cyclodextrin

We have already answered the primary question about the MS method performances. The statistical significant parameters unambiguously underline a superior accuracy ($r = 1$). It must be obvious that the D_{SD} data allows for a high selective analysis of CDs in mixture within low *m/z* values. Let us compare D_{SD} data on γ–CD under conditions A_1 and B_1 (Table AS1). The analysis of D_{SD} data of the same ions of α– and β–CD is carried out. The chemometric results are summarized in Tables AS13 and AS14 as well as Figs. AS26 and AS27. Fig. AS28 tackles the correlation among D_{SD} parameters. The analysis distinguishes between CDs by pairs, from the perspective of the chemometrics. What is crucial is that, as aforementioned, the three analytes exhibit identical *m/z* values within the range $m/z = 100$–200 (Fig. AS25) and a quantification on the base on MS peak position unable to detect selectively these analytes in mixture. However, by D_{SD} parameters, a significant statistical selectivity of CDs in low *m/z*–range of the spectra is achieved.

3.5. Stochastic dynamic mass spectrometric diffusion parameters of β–cyclodextrin – Atmospheric pressure chemical ionization mass spectrometric data

Having documented the capability of Eq. (1) to determine highly accurately, precisely and selectively the CDs within low *m/z*–region of the spectra we shall move in this subsection to an important analysis of β–CD under APCI–MS experimental conditions (Fig. AS10, experiments 01–06). A correlation between ESI– and APCI–MS D_{SD} data shall be carried out. Fig. AS29 depicts the temporal behavior of MS ions of six independent measurements 01–06 over overlapped spans of scan time.

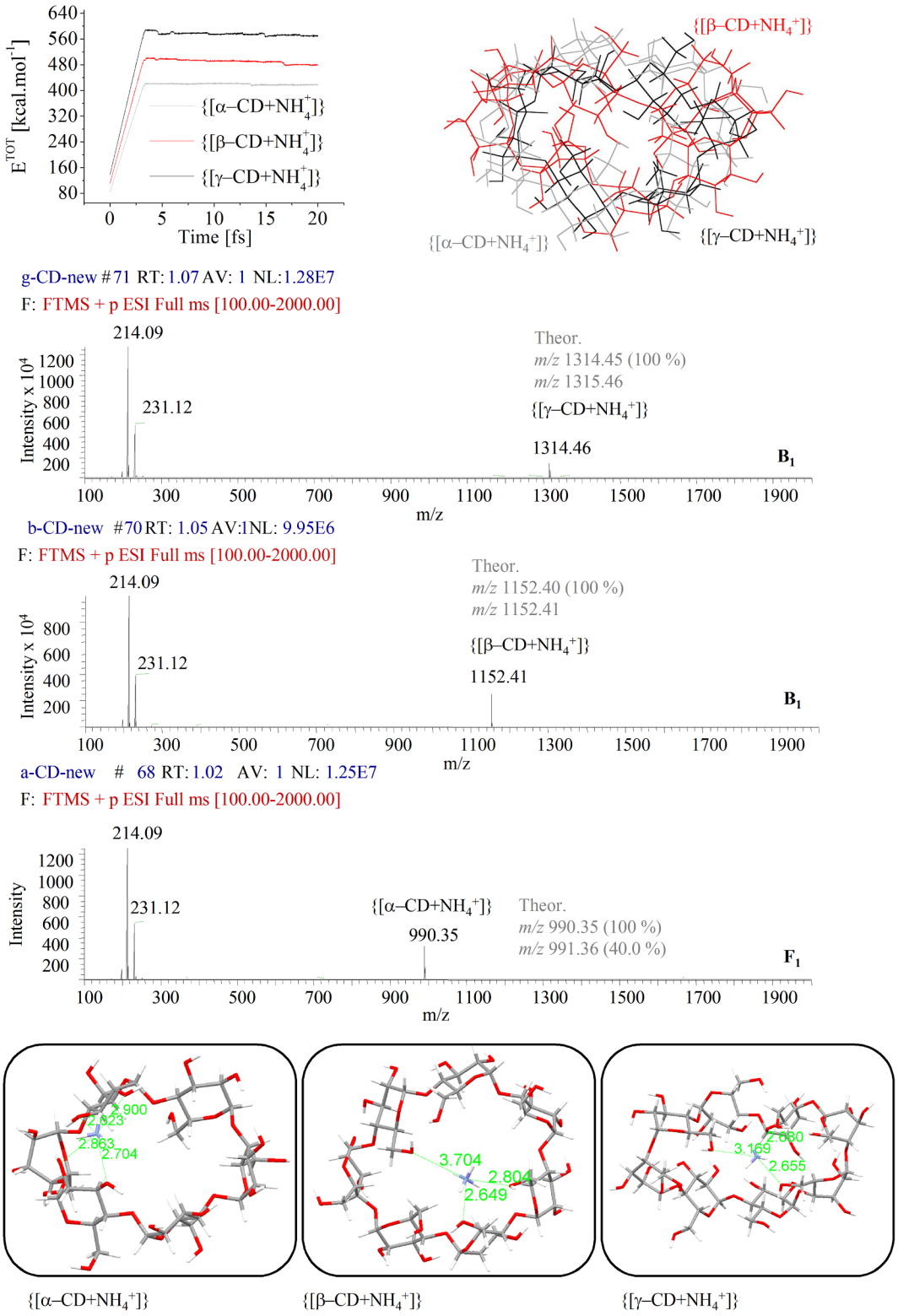

Fig. 3. ESI(+)–MS spectra of CDs; molecular dynamic energetic: total energy (E^{TOT}) [kcal·mol^{-1}] *versus* time [fs]; 3D molecular conformation of ammonium adducts of analytes; intermolecular/ionic hydrogen bonds (bond lengths [Å]).

Fig. AS30 presents ion currents with respect to time; the functional relationship $(I–\langle I\rangle)^2 = f(t)$ and its nonlinear approximation to SineSqr function. Tables AS15 and AS16 summarize absolute MS intensity with respect to different spans of time, D_{SD} parameters and statistical parameters. There should be linear correlation between D_{SD} parameters of APCI– and ESI–MS data; and among APCI–MS data on experiments 01–06 looking at the overlapped spans of time (Fig. AS31). There has been evidenced experimentally not only high accuracy of ESI– and APCI–MS data, but also high selectivity of CDs within low *m/z*–region of the spectra.

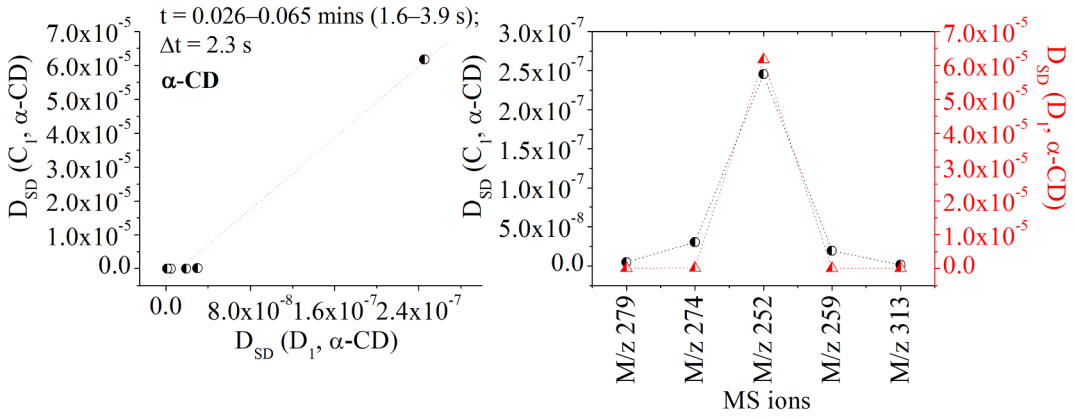

	Value	Error	*r*	SD	N	*p*
A	-3.4592.10^{-6}	1.8494.10^{-6}	**0.99403**	3.47381.10^{-6}	5	5.53175.10^{-4}
B	263.1085	16.67297				

Fig. 4. Relations among D_{SD} [$cm^2 \cdot s^{-1}$] parameters of MS ions of α–CD within *m/z* 100–500 of experiments E_1/F_1 and C_1/D_1; chemometrics; D_{SD} parameters [$cm^2 \cdot s^{-1}$] of experiment C_1 belonging to each of the shown MS ions are given in "black," while those from experiments D_1 – in "red."

3.6. Temperature dependence of the stochastic dynamic diffusion parameters of cyclodextrins

Judging from the results from application of formula (2) to quantify the temperature dependency on the MS intensity with respect to the two independent ESI– and APCI–MS measurements depicted in Fig. CS3 there appears to be excellent linear relation ($r = 0.98_{27}$).

3.7. Theoretical data

3.7.1. Molecular conformations and electronic structures of mass spectrometric fragment ions

Not being able to encompass all aspects of conformational analysis and electronic effects of CBs, due to, flexibility of their molecular structures. Moreover, an almost identical proton accepting ability of O–centres of OH–groups and diversity of intra– and intermolecular hydrogen bonds of monomers, oligomers and polymers occur. Thus, this subsection focuses on molecular structure of MS ions within low *m/z*–region of the spectra aiming at correlating among 3D conformations, subtle electronic effects and D_{QC} parameters. Fig. 6, BS26 and BS27 depict molecular optimization of species and their energetics obtained by *ab initio* and DFT–MD methods. A question that has to be addressed is whether we can expect the D_{QC} parameters to correspond excellent with D_{SD} parameters taking into consideration that the CDs are characterized by flexible molecular structures. They stabilize closely disposed as energetic conformational situations. In order to, make our claims plausible, we describe energetic of different molecular conformations belonging to each experimental MS ion. CBs tend to form moderate–to–weak intramolecular OH···O(H) hydrogen bonds. In the case of MS ion at *m/z* 198, molecule of (1) interacts with NH_4^+ cation *via* NH_4^+···O(H) intermolecular hydrogen bonds (*r*(N···O) = 2.591 and 2.637 Å). In seeking to understand the governing forces and molecular factors determining the TD stability of MS species within different positional isomers we have carried out systematically evaluation of

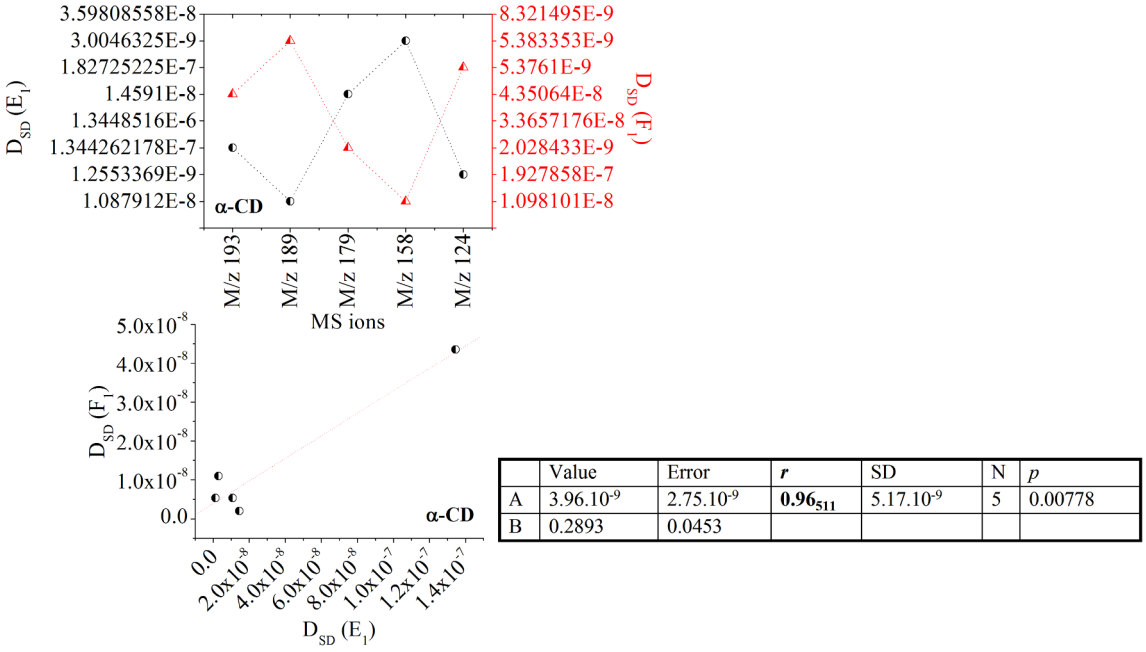

	Value	Error	*r*	SD	N	*p*
A	3.96.10^{-9}	2.75.10^{-9}	**0.96$_{511}$**	5.17.10^{-9}	5	0.00778
B	0.2893	0.0453				

Fig. 5. Relations among D_{SD} parameters of MS ions of α–CD within *m/z* 100–500 of experiments E_1/F_1; chemometrics; D_{SD} parameters [$cm^2 \cdot s^{-1}$] of experiment E_1 belonging to each of the shown MS ions are given in "black," while those from experiments F_1 – in "red."

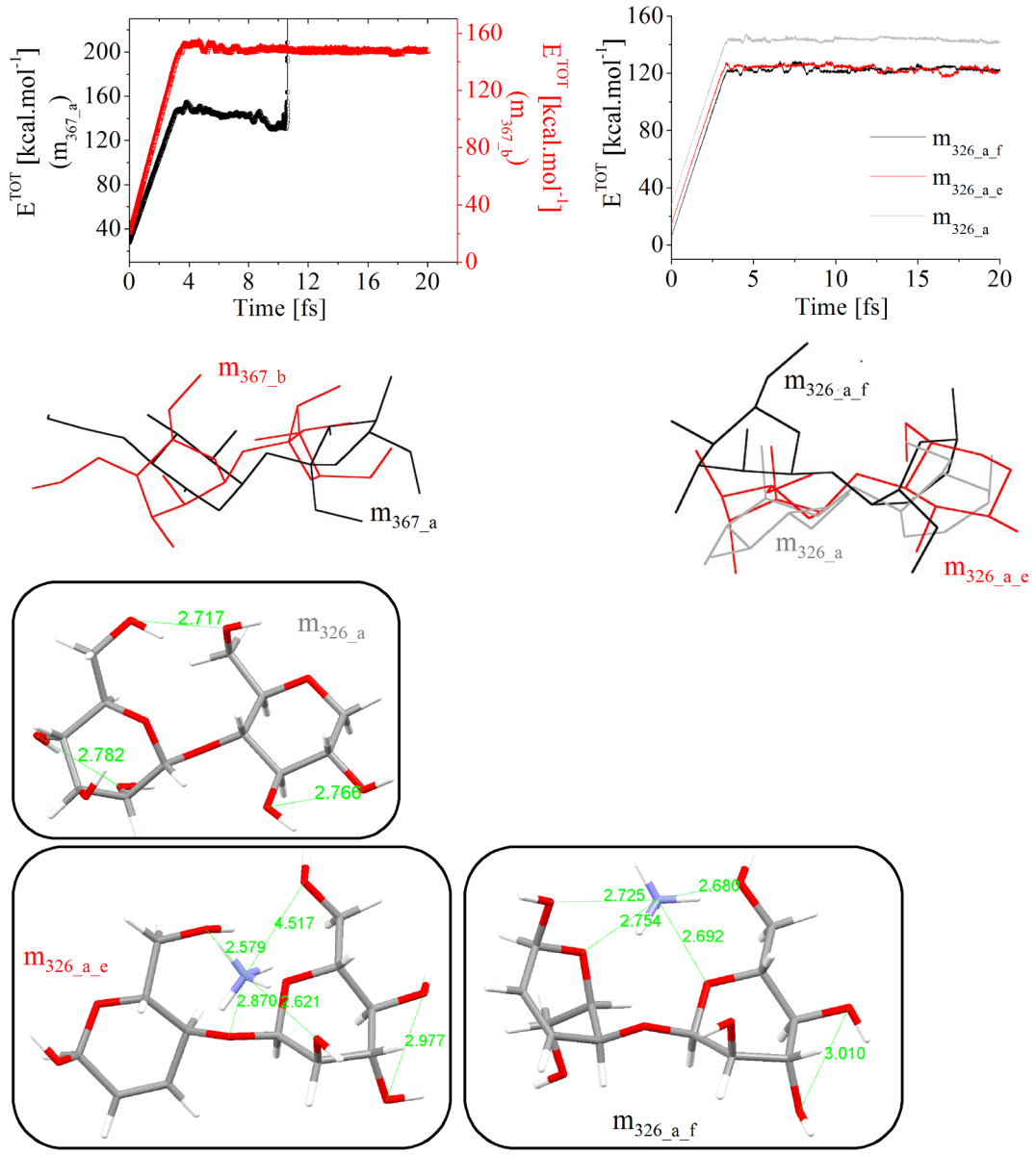

Fig. 6. Molecular dynamics of acyclic dimeric carbohydrate ions at *m/z* 367 and 326; total energy (E^{TOT}) [kcal·mol^{-1}] *versus* time [fs]; 3D molecular conformations and intermolecular/ionic hydrogen bonds (bond length [Å]).

energetics of ions (Figs. BS2–BS12). The criterion is very sensitive toward any conformational change or subtle electronic effects. Let us describe the energetics of species m_{155_a} to m_{155_c} and m_{171_a} to m_{171_d}. Most stable are cations m_{151_b} and m_{171_c} (ΔE^{TOT} = |9.0316| and |12.0931| kcal·mol^{-1}). In parallel, one further question is whether the size of CD ring affects on TD of ions within competitive fragment paths of analytes (3)–(5). In other words, is there significant difference in energy of given ions, for example, m_{198_a} and m_{198_b} with respect to analysis of isolated analytes or analytes in mixture? Fig. BS26 only indicates a difference in total energy ΔE = |0.00174015| a.u. The same is true for cations m_{231_a} and m_{231_b}, where the cation containing 2,5-bis-hydroxymethyl-tetrahydro-furan-2,3,4-triol appears more stable comparing with charged species containing a six–membered cyclic CB fragment 6-hydroxymethyl-tetrahydro-pyran-2,3,4,5-tetraol. Even studying only MS spectra of (5) there is assumed an intramolecular rearrangement leading to a transition $m_{198\_a} \rightarrow m_{198\_b}$. Nevertheless, within the series of MS m_{362_c} and m_{362_d} ions the latter one contains disaccharide scaffold, however, with a mixed 5– and 6–membered ring containing monomeric units it appears less favourable from the TD point of view. The NH_4^+ and Na^+ adducts are very stable cationic ensembles of CBs comparing with the charged CBs themselves.

3.7.2. Quantum chemical diffusion parameters

3.7.2.1. Quantum chemical diffusion parameters of monomeric and acyclic oligomer carbohydrates – a correlation between experiment and theory. The next analytical step lies in determining D_{QC} parameters. The thermochemistry of GS and TS are summarized in Table BS5. Tables BS6–BS8 represents atomic coordinates of MS species in the two states; vibrational frequencies and ionization potentials. The determination of TSs is obtained by *ab initio* and DFT–MD using BO approximation (Fig. BS27). There is excellent correlation with a significant coefficient of correlation between D_{SD} and D_{QC} parameters (Fig. BS28). In order to, illustrate the great sensitivity and selectivity of the D_{SD} parameter let us describe D_{QC} parameters of different molecular conformations and isomers of MS ions. How these values fit to experimental D_{SD} parameters? Ions m_{113} and m_{113_a} show $D_{QC} = 333.31_{66}$ and 74.06_{15}, while ions m_{198_a} and m_{198_b} reveal $D_{QC} = 187.95_{067}$ and 348.32_{8}. The significant differences in values enable us to distinguish precisely

among 3D molecular conformations and electronic structures of an ion by comparing D_{QC} with D_{SD} data. The analysis of ions m_{120_a} and m_{214_a} yields to D_{SD} = 1005.6 and 90.75_{36}. As the latter figure indicates, the D_{QC} of the ions *m/z* 113 and m_{198_b} correlate with experimental D_{SD} parameters. This agrees well with known experimental assignment [51,52]. The D_{SD} parameters can be used as highly accurate and sensitive elicitation tool to distinguish among a large series of ions exhibiting subtle changes of electronic or molecular 3D structures or both. The analysis of D_{SD} and D_{QC} values shows excellent coefficients of correlations $r = 0.99_{981}$ and 0.99_{951}.

3.7.2.2. Quantum chemical diffusion parameters of native cyclodextrins – a correlative analysis between experiment and theory. We have to determine correlation among D_{SD} parameter of ions within *m/z* = 100–500 and D_{QC} data. The most stable 3D molecular and electronic structures of MS ions depending on their proton accepting ability and charge localization should be obtained. Fig. BS32 depicts DFT energetics of ions. The D_{QC} parameters are obtained namely using the most stable conformation of the ions from the perspective of the chemical TD (ions m_{141_d}, m_{158_d} and m_{171_b}). The determination of TS is carried out by MD analysis (Fig. BS33). The molecular vibrations of GS and TS are summarized in Table AS17. Table AS18 and AS19 show thermochemistry. The correlations between D_{SD} and D_{QC} values are (Fig. AS14) almost perfect linearly. The γ–CD shows $r = 0.9963_9$ (Fig. AS34). We turn to discuss, therefore, controversy the view that the MS does not provide multidimensional structural information [41,51]. However, such line of though does not reflect the real capability of the method. We provide an affirmative empirical proof of our claim that the MS is able not only to provide highly accurate and precise quantitative data, but also exact 3D and electronic structures of the molecules.

4. Discussion

The high selectivity and sensitivity of the D_{SD} parameters are, namely, the key point to understand why model Eq. (1) has significant affect on development *into* quantitative methodology base on soft ionization mass spectrometry. Because of, the MS intensity reflects 3D structure of the molecular ion, however, to any MS ions at any *m/z* value a set of different 3D molecular and electronic structures of analytes depending on experimental conditions can occur. The scan time does not affect the *m/z* value. However, it affects the intensity of the MS peaks of analyte ions, due to perturbation of their 3D molecular and electronic structures during the experiment over different spans of time. Different size CDs exhibit different inters ionic interactions and fragment reactions. Given that, the products of interactions of CDs at high *m/z* values interact differently, thus, affecting the electronic structures and molecular conformations of common products of fragment paths at low *m/z* values. In spite of, that the latter ions exhibit identical *m/z* values, the intensity of the analyte ions can de different depending on experimental conditions, in context chemical composition of the MS continuum. Through the common claim that MSs unable to determine quantitatively CDs on the base on analyte ions at low *m/z* values, our analysis of D_{SD} parameters and application of Eq. (1) to treat the MS intensity throw light on that such claim is true only looking on experimental MS parameter *peak position* or *m/z*–value. The experimental MS spectra, however, are significantly more informative looking at methods for quantifying the outcome *intensity*. As we could expect, under identical experimental conditions and spans of scan time, the D_{SD} parameters correlate excellent linearly (Figs. 4 and 5). The coefficients of correlations vary from 0.99_{403} to 1. How can such excellent statistical parameters obtain looking at method performances discussed in Section 3.1? It would seem that the proper place to seek for an answer to this question is the background of the SD concept, which we have used to derive Eq. (1). Our theory [19–26] is based on SD description of the MS measurable parameter *intensity*. It is carried out within the probability theories [44], studying the so–called *fluctuations* of stochastic variable, in this case – the *intensity* of a MS ion with respect to the scan time. However, the connotation of the word *probability* in the modern stochastic theories is *physical probability* (frequency-based probabilities) or *evidential probability*, rather than *indifference* when we are talking about *equal probability* [44]. In this context, we use *plausibility theories,* rather than *probability theories* in describing stochastic processes. The frequency-based probabilities account for the so–called *true frequency* or *true probability*. Looking at experimental MS measurements of the *intensity* with respect to the scan time the theory hypothesizes a true value of the MS intensity to which a set of repeatedly obtained values within an infinite number of experimental measurements would converge. On the other hand, it is notoriously that the MS intensity is approximated to concentration of analyte ion [25]. The concentration limits of detection of the method are $\sim 10^{-9}$–10^{-12} mol·L^{-1}, which corresponds to $\sim 10^{16}$–10^{13} numbers of particles. In parallel, the fluctuations of the number of the particles, which as has been said, corresponds to MS intensity. It is given by the so–called $(N)^{1/2}$–law [45]. Thus, the fluctuation of the intensity should figure on fluctuation of the number of particles within $(N)^{1/2}$ values $\sim 10^8$–10^6. The accuracy of MS measurement does not account for fluctuations of $\sim 10^6$ particles. The stochastic plausibility theories describe exactly the phenomena, in this case, the temporal behavior of MS intensity from the perspective of empirical measurements. The Ornstein–Uhlenbeck and Box–Müller methods are exact methods [45,46]. The derivation of the latter method can be found in [47,48], while more detail on the former approach – in [47,49,50]. Therefore, Eq. (1) is an exact equation. This appears to be an explanation why not only in this work, but also in other studies, so far [19–26], the correlations among D_{SD} data yield to good–to–excellent statistical parameters. Perhaps, one might assume that only this explanation is not straightforward, accounting for that the newcomers of instrumentation developments of MS provide ultra-high resolving power, accuracy and precision of measurements. Such argument, as can be expected, is justified from the perspective of search of empirical proofs of validity of Eq. (1). Moreover, as has been shown [19–26] D_{SD} parameter reflects a 3D molecular conformation and accounts for subtle electronic effects within an electronic multidimensional structure and correlation with D_{QC} parameters. Because of, according to our description of *fluctuation* of MS intensity with respect to a span of scan time, we look at inherently arising fluctuations of intensity, due to, perturbation or change of the 3D conformation or electronic structure of the ions. The order of magnitude of the latter inherently arised *fluctuations* due to perturbation of the molecular structure are significantly higher than the order of magnitude of fluctuations due to number of analyte molecules. Thus, perturbation or change of the multidimensional molecular structure is MS detectable. By contrast, the fluctuation of the intensity, due to, number of particles does not appear detectable, experimentally. It does not contribute to error of measurement of the intensity and is not taken into consideration in Eq. (1). In addition, one of the significant advantages of the latter formula, among others, is that it quantifies experimental intensity having an order of magnitude $\sim 10^6$ (Table CS2, Appendix C). In parallel, the error contribution of noise is $\sim 10^2$ (Fig. CS2). The error of the measurements affects significantly the *m/z*–values comparing with their insignificant affect on the MS intensity (Tables CS1 and CS2). The arguments that the SD theories appears exact description of MS phenomena, and, in parallel, the MS methods provide superior instrumental performances allow for classifying the determined multidimensional structure on the base on our theoretical concept as an *exact* or *absolute* 3D structure. Moreover, the quantum chemical methods also provide high accuracy of energetic of the molecular systems.

A next point is correlation between D_{SD} parameters and D_{CMM} data obtained on the base on the *current monitoring method* (Eq. (10) in [24]). Thus, we verify the validity of our formula by means of independent as methodologic approach. The D_{SD} parameters of α–CD fit excellent with D_{CMM} ones (Fig. AS21) and show $r = 0.98_{143}$.

Further comment on our theory is associated with applicability of

the model relations to different mass spectrometers. As far as, our method has been tested, so far, using analytical instrumentation operating with 3Q-trap and Orbitrap analyzers, the following question logically arises: do equations depicted in Fig. 1 applicable to mass spectrometers operating with Q-TOF analyzer as a broadly implemented in the analytical practice instrumental scheme, among others, including for analysis of biomacromolecules [53]? In order to address this question we propose to look at the background of the latter method, which provides direct information about the mobility of MS ions [54]. The ion mobility is directly connected with the diffusion and, thus, it is correlated with our D_{SD} data. However, it must be stressed that when the analytes are biomacromolecules, the Einstein's relation, which very frequently has been adopted studying diffusion phenomena [54] cannot be applied. The same is true for analysis of short spans of scan time according to our concept. This drawback of the Einstein's relation is overcome by applying our method [19–26]. Because of, the results from this work confirm that it appears applicable to different spans of scan time, in spite of, molecular weights of analytes. Moreover, we have shown by model Eq. (2) that diffusion phenomena under ESI–MS experimental conditions are quantify with excellent coefficient of statistical correlation when is used our empirical modification of fluctuating force in the forward Fokker–Planck equation applied to an Ornstein–Uhlenbeck process (see Eq. (5) [26]). Therefore, we follow up with an assumption that TOF MS outcomes should be quantified highly accurately by Eqs. (1) and (2). A direct link of the ion mobility with diffusion parameters of the ions according to the later formulas and 3D structures of the analyte species is itself logical.

A final point to notice is that the evaluation of *reproducibility* and *sensitivity* of MS variable *intensity* from the perspective of the chemometrics needs to employ namely Eqs. (1) and (2). Because of, as has been evidenced empirically the absolute value of the total MS intensity within the whole span of the scan time of experiment represents a sum of the intensity values *per* different spans of the scan times, but this change of intensity value is a result from the change of the molecular conformation or perturbation of the electronic structures (Fig. BS21). Therefore its quantification should be based on parameter which accounts for the 3D molecular and electronic structures like the D_{SD} parameter and formula (1). There is unable to account precisely for the fluctuations of the MS intensity using directly the statistical tests over the whole span of the measurement time. The same is true for the chemometric treatment of the *m/z*–values, because of according to the SD concepts used to derive Eqs. (1) and (2), the characteristic functions accounting for the drift and diffusion in the forward Fokker–Planck equation are mutually connected [26,45]. According to our empirical modification of the latter function which fits excellent to the experiment, however, there is included the mass of the analyte ion (m) (Eq. (5) [26] and Section 3.6) It is self–evident, therefore, that a precise chemometric analysis of experimental MS outcomes should be carried out *per* concrete spans of the whole scan time of measurement according to the discussed formulas. In addition, as the results from Ref. [26] and Section 3.6 show, our formulas (1) and (2) are applicable to different schemes of mass spectrometers and, despite, the molecular masses of the analytes.

5. Conclusion

With the shown still in the "Abstract' to this work summary of among the most important results from our study, it becomes easy to understand the significance of this contribution to the methodological development of the soft–ionization methods of the mass spectrometry, underlying their application to 3D conformational and electronic structural analyses, in particular, focusing the attention on native cyclodextrins and their mixtures with simple monomeric and acyclic oligomer carbohydrates; and owing to the fact that the structural analysis of these derivatives represent significant analytical challenge. The paper has presented successfully a completely new approach to treat quantitatively the mass spectrometric measurable outcome intensity, which *via* our model equations and the so–called *stochastic dynamic diffusion parameter* "D_{SD}" provides direct connection with multidimensional structures of analytes. One particular advantage of our approach together with the high selectivity, sensitivity and precision of the D_{SD} data is that the parameter accounts for the effect of the temperature on the 3D molecular and electronic structures of the CDs, in particular, and carbohydrates, in general. Owing to that these objects show competitive proton accepting ability of the O–centres and a diverse number of intra– and intermolecular hydrogen bonds of monomers, oligomers or polymers, our method provide unique opportunity to detail quantitatively ad structurally the noncovalent interactions and their effect on 3D molecular conformation and electronic structures of molecules, in particular, highlighting the effect of the temperature as major environmental factor determining the hydrogen bond networks.

Acknowledgements

We are grateful to Deutscher Akademischer Austausch Dienst (Germany) for a grant within the priority program "Stability Pact South-Eastern Europe"; the Alexander von Humboldt Stiftung; the Deutsche Forschungsgemeinschaft; the central instrumental laboratories for structural analysis at Dortmund University (Federal State Nordrhein–Westfalen) and analytical and computational laboratory clusters at the Institute of Environmental Research at the same University (Project number: 224755478). The work was carefully carried out. Nevertheless, authors and publisher do not warrant the information therein to be free of errors. It is being published in English aiming at a widest access to the scientific contributions. English is not native language of the authors, however. Stylistic rough edges might occur. The authors hope for understanding of the reader.

Appendix A. Supplementary material

Supplementary data to this article can be found online at https://doi.org/10.1016/j.bioorg.2019.103308.

References

[1] S. Bai, X. Zhang, X. Ma, J. Chen, Q. Chen, X. Shi, M. Hou, P. Xue, Y. Kang, Z. Xu, Biomater. Sci. 6 (2018) 3126.
[2] M. Pei, J. Pai, P. Du, P. Liu, Mol. Pharmaceut. 15 (2018) 4084.
[3] R. Cole (Ed.), Electrospray and MALDI Mass Spectrometry: Fundamentals, Instrumentation, Practicalities, and Bioloical Applications, 2010, Wiley, Hoboken, New Jersey, pp. 1–845.
[4] J. Gross (Ed.), Mass Spectrometry, 3rd ed., 2017, Springer Verlag, Berlin Heidelberg, pp. 1–968.
[5] R. Zenobi, Anal. Chem. (2017), https://doi.org/10.1021/acs.analchem.5b01062.
[6] B. Ivanova, M. Spiteller, Int. J. Biol. Macromol. 87 (2016) 263.
[7] B. Ivanova, M. Spiteller, Int. J. Biol. Macromol. 64 (2014) 383.
[8] C. Klein, S. Cologna, R. Kurulugama, P. Blank, E. Darland, A. Mordehai, P. Backlund, A. Yergey, Analyst 143 (2018) 4147.
[9] Y. Fan, S. Lu, J. Cao, Int. J. Mass Spectrom. 435 (2019) 163.
[10] L. Ruhaak, G. Xu, Q. Li, E. Goonatilleke, C. Lebrilla, Chem. Rev. 118 (2018) 7886.
[11] S. Lee, S. Valentine, J. Reilly, D. Clemmer, Int. J. Mass Spectrom. 309 (2012) 161.
[12] A. Pana, L. Rusnac, G. Bandur, M. Silion, C. Deleanu, M. Balan, e-Polymers, 2011, no. 004, ISSN 1618-7229.
[13] M. Sarbu, Z. Vukelic, D. Clemmer, A. Zamfir, Analyst 143 (2018) 5234.
[14] J. Carroll, C. Lebrilla, Org. Mass Spectrom. 27 (1992) 639.
[15] F. Pepi, A. Ricci, S. Garzoli, A. Troiani, C. Salvitti, B. Rienzo, P. Giacomello, Carbohydrate Res. 413 (2015) 145.
[16] N. Leymarie, J. Zaia, Anal. Chem. 84 (2012) 3040.
[17] K. Khatri, Y. Pu, J. Klein, J. Wei, C. Costello, C. Lin, J. Zaia, J. Am. Soc. Mass Spectrom. 29 (2018) 1075.
[18] J. Zaia, Mass Spectrom. Rev. 23 (2004) 161.
[19] B. Ivanova, M. Spiteller, Quantification by Matrix-Assisted Laser Desorption Ionization Mass Spectrometry Using An Approach Based On Stochastic Dynamics. Experimental And Theoretical Correspondences, GRIN Verlag, Muenchen, 2018, pp. 1–86, ISBN: 9783668703179.
[20] B. Ivanova, M. Spiteller, M. An Experimental and Theoretical Mass Spectrometric Quantification of Non–covalent Interactions in High Order Homogeneous Self–associates of Nucleobases and Nucleosides, NOVA Science Publisher, New York, 2018, pp. 1–134, ISBN: 9781536142433.
[21] B. Ivanova, M. Spiteller, J. Mol. Struct. 1173 (2018) 848.

[22] B. Ivanova, M. Spiteller, Experimental mass spectrometric and theoretical treatment of the effect of protonation on the 3D molecular and electronic structures of low molecular weight organics and metal–organics of silver(I) ion, Nova Science Publishers, N.Y., 2019, pp. 1–182 ISBN: 978-1-53614-886-2.
[23] B. Ivanova, M. Spiteller, Mass Spectrometric Experimental and Theoretical Quantification of Reaction Kinetics, Thermodynamics and Diffusion of Piperazine Heterocyclics in Solution, in: J. Taylor (Ed.), Advances in Chemistry Research, vol. 48, NOVA Science Publishers Inc., Publisher, N.Y., 2019, pp.1–82, ISBN: 978-1-53614-724-7.
[24] B. Ivanova, M. Spiteller, J. Mol. Struct. 1179 (2019) 192.
[25] B. Ivanova, M. Spiteller, J. Mol. Liquids 282 (2019) 70–87.
[26] B. Ivanova, M. Spiteller, J. Mol. Liquids 292 (2019) 111307.
[27] B. Ivanova, M. Spiteller, Analyst 137 (2012) 3355–3364.
[28] C. Kelley, Iterative methods for optimization, SIAM front, Appl. Math. 18 (2009).
[29] M. Otto, Chemometrics, third ed., Wiley, Weinheim, 2017, pp. 1–383.
[30] Apache OpenOffice, http://de.openoffice.org.
[31] K. Madsen, H. Nielsen, T. Tingleff, Informatics and Mathematical Modelling, second ed., DTU Press, 2004.
[32] J. Miller, J. Miller, Statistics and Chemometrics for Analytical Chemistry, Pentice Hall, London, 1988, pp. 1–271.
[33] J. Taylor, Quality Assurance of Chemical Measurements, Lewis Publishers, Inc., Michigan, 1987, pp. 1–328.
[34] V. Taylor, R. March, H. Longerich, C. Stadey, Int. J. Mass Spectrom. 243 (2005) 71.
[35] Y. Tan, N. Polfer, J. Am. Soc. Mass Spectrom. 26 (2015) 359.
[36] M. Zhang, Z. Geng, Y. Yu, Energy Fuels 25 (2011) 2664.
[37] M. Zhang, Z. Geng, Y. Yu, Comput. Theor. Chem. 1067 (2015) 13.
[38] T. Uto, T. Yui, ACS Omega 3 (2018) 8050.
[39] C. Shao, K. Shi, Q. Hua, L. Zhang, Y. Dai, W. You, Y. Liu, C. Li, C. Zhang, J. Mol. Model. 24 (2018) 124.
[40] M. Stas, J. Chudoba, M. Auersvald, D. Kubick, S. Conrad, T. Schulzke, M. Pospísil, J. Anal. Appl. Pyrol. 124 (2017) 230.
[41] K. Song, R. Spezia, Theoretical Mass Spectrometry, De Gruzter, Berlin-Boston, 2018, pp. 1–228.
[42] H. Pilath, M. Nimlos, A. Mittal, M. Himmel, D. Johnson, J. Agric. Food Chem. 58 (2010) 6131.
[43] E. Gaidamauskas, E. Norkus, E. Butkus, D. Crans, G. Grinciene, Carbohydrate Res. 344 (2009) 250.
[44] P. Schuster, Stochasticity in Processes, Fundamentals and Applications to Chemistry and Biology, Springer Verlag, Berlin Heidelberg, 2016, pp. 1–718.
[45] D. Gillespie, Phys. Rev. E (1996) 2084–2091.
[46] G. Uhlenbeck, L. Ornstein, Phys. Rev. 36 (1930) 823.
[47] D. Gillespie, Markov Prosesses, Academic Press, N.Y., 1992, pp. 1–566.
[48] A. Satoh, Introduction to Practice of Molecular Simulation, Elsevier, Amsterdam, 2011, pp. 1–223.
[49] E. Nelson, Dynamic Theories of Brownian Motio, Princeton University Press, N.J., 1967, pp. 1–142.
[50] W. Coffey, Y. Kalmykov, J. Waldron, The Langevin Equation, World Scientific Publishing, N.J., 2004, pp. 1–679.
[51] T. Veenstra, Biophys. Chem. 79 (1999) 63.
[52] M. Gaye, R. Kurulugama, D. Clemmer, Analyst 140 (2015) 6922.
[53] V. Gabelica, S. Livet, F. Rosu, J. Am. Soc. Mass Spectrom. 29 (2018) 2189.
[54] H. Tseng, T. Jen, K. Peng, S. Chen, Appl. Phys. Lett. 84 (2004) 1456.